

# Feasibility of Wearable Armband Bipolar ECG Lead-1 for Long-term HRV Monitoring by Combined Signal Averaging and 2-stage Wavelet Denoising

Omar J Escalona, Sophie Magwood, Anna Hilton and Niamh McCallan

Ulster University, School of Engineering, Belfast, UK

## Abstract

*Heart rate variability (HRV) is a clinically important and prominent cardiovascular diseases diagnostic factor. Since HRV is a highly individualised measure, long-term continuous ECG and HRV tracking using a non-invasive armband-based wearable monitoring device is an appealing option for HRV trend-based indicator of general health. Therefore, we investigated the correlation between the bipolar arm-ECG Lead-1 (electrodes axis coplanar to chest and at axilla level) HRV measurements and their corresponding standard measurements from the standard chest ECG Lead I, using a 2 stage dB4 Wavelet-based denoising process supported by an iterative signal-averaged ECG optimal-thresholding adaptation algorithm on the arm-ECG signal, followed by a Pan-Tompkins QRS-detection algorithm. The conventional Pearson correlation coefficient was used as the main performance assessment metric. Four clinically common HRV time-domain metrics were studied: SDNN, RR-rms, RR-median and the interquartile-range value of normal-to-normal heartbeat intervals (IQRNN). The results revealed that RR-rms and RR-median HRV metrics from bipolar arm-ECG (Lead-1) closely correlated to the values measured from the standard Lead-I and present potential for clinical use.*

## 1. Introduction

In the United Kingdom, it is estimated that 7.6 million people are living with a heart or circulatory related disease. Improved survival rates alongside a growing population means this number is likely to increase [1].

Due to the growing pressure on health services in recent years a need for at home health monitoring devices has become even more prevalent [2]. One area of growth in at-home medical devices is in those used to monitor cardiac electrical activity; Electrocardiograph (ECG) recording.

Heart failure (HF) is the inability of the heart to effectively pump blood to the body [3]. The autonomic nervous system (ANS) can be broken down into two different sections, the sympathetic nervous system and the parasympathetic nervous system. Normally the two

nervous systems perform their activities at a dynamic equilibrium [3]. Critical states of HF can be revealed by the ECG signal Heart Rate Variability (HRV) analysis and monitoring methods [3]. HRV is a clinically important and prominent cardiovascular diseases diagnostic indicator, and useful for the detection of cardiac autonomic modulation and diabetes mellitus states leading to cardiovascular autonomic neuropathy complications [3]. Basically, HRV extracted from an ECG reveals variations of inter-beat-interval (IBI) of normal-to-normal heart beats time series [4]: providing useful information on the behavior of heartbeats for diagnostic purposes. Since HRV is a highly individualised measure [4], long-term continuous ECG, and hence, HRV tracking using a non-invasive and user convenient armband-based wearable monitoring device would be an appealing option for HRV trend-based indicators of general health.

In recent years Discrete Wavelet Transform (DWT) has become a useful signal processing technique for signals overcoming common noise issues in ECG signal, such as internal muscle movement and powerline interference which can disrupt the ECG signal [5].

In this study we investigated the correlation between the bipolar arm-ECG Lead-1 (electrodes pair axis coplanar to chest and at axilla level) [5] HRV measurements and their simultaneous (in same subject) correlation with measured HRV values from the standard Lead-I ECG (chest). This was achieved by implementing a 2 stage Daubechies 4 wavelet decomposition (Db4) discrete wavelet-based denoising process, supported by a signal-averaged ECG (SAECG) based embedded adaptive ECG signal case noise sigma ( $\sigma$ ) determination algorithm for optimal Db4 thresholding, using a Single Fiducial Point (SFP) QRS alignment technique [6] for the SAECG denoised signal referencing process, and the conventional Pan-Tompkins QRS detection algorithm [7] for extracting the IBI time-series for various HRV time-domain metrics comparative assessment: Arm-ECG Lead-1 vs chest Lead I ECG values.

## 2.0 Methods

### 2.1 Arm-ECG Data

From an initial clinical study conducted at the Craigavon

Area Hospital (Northern Ireland), WASTCARd arm-ECG mapping database [5], a reduced set of ten patient cases were extracted from this original larger database based on the simple criterium of: all those who had a similar body-mass-index (BMI) of  $25 \text{ Kg/m}^2 \pm 2\%$ , and consequently, similar arm circumference of  $28.5\text{cm} \pm 3\%$  (SD), using the linear regression model equation [8] between BMI and the estimated mid-upper arm circumference (MUAC) value.

Table 1, presents the patients set baseline demographic characteristics. There, 77% of the patients included in this pilot study were female (33% male), and the mean BMI value of the 10 subject cases was  $24.87 \pm 0.26$  (SD)  $\text{Kg/m}^2$ . ECG recordings were taken at rest for 8 minutes duration.

Table 1. Selected dataset patients' baseline demographics.

Case Number	Age / Years	Gender	Weight / Kgs	BMI / $\text{Kg/m}^2$	MUAC / cm
1	68	F	68.0	25.28	29.01
2	56	F	61.0	24.75	28.40
3	37	F	68.4	24.53	28.14
4	67	F	66.0	24.84	28.50
5	52	F	64.5	24.58	28.20
6	29	M	61.9	25.11	28.81
7	41	F	53.3	24.67	28.30
8	31	M	82.2	24.82	28.47
9	33	F	72.0	24.91	28.59
10	22	M	86.2	25.19	28.90
Mean	43.6		68.35	24.87	28.53
Standard Deviation	16.22		9.81	0.26	0.29

HRV metrics of the standard chest ECG Lead I provided the “gold standard” of the HRV values, in each patient case, for assessing the feasibility of HRV values measured from the bipolar Arm Lead-1, by computing the correlation coefficient (p) and linear regression model coefficient of determination, in a scatter plot of dataset pairs.

## 2.2 Two-stage Db4 wavelet-based denoising

All ECGs are first passed through a DC removal 1<sup>st</sup> step, followed by Butterworth bandpass, 0.5 - 40 Hz, 4<sup>th</sup> order [5] and notch filters as a preliminary denoising process, before applying the proposed two-stage Db4 wavelet-based denoising strategy. Prior to the 1<sup>st</sup>-stage of the Db4-based denoising process (Fig.1), the prefiltered ECG signal sigma noise value for optimal Db4 thresholding is searched systematically (at  $\sigma$  incremental steps of 0.15, for 30 values of  $\sigma$ ). The  $\sigma$  value yielding the Db4 maximum ECG denoising performance, using the 700 ms SAECG window from 600 beats as the noiseless P-QRS-T ECG reference (gold standard) signal component to assess noise level at every incoming P-QRS-T, in a beat-by-beat basis, for each individual case; by the following Matlab coded operations:

`q = currentBeatNumber; % Beat-by-beat; q index: from 1 to 600`  
`noise = saecg700win - ECGdb4waveletdenoised700win(q);`

The optimal  $\sigma$  value gives a maximum mean SNR vector:

`SNR700vector(q) = mean(saecg700win.^2)/mean(noise.^2);`

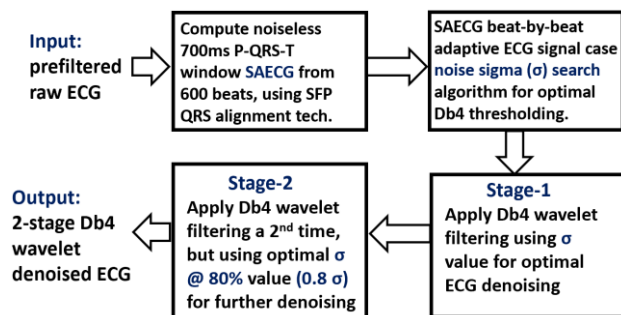


Figure 1. Algorithm flowchart for the 2-stage ECG Db4 denoising process.

Table 2 presents the resulting optimal  $\sigma$  values for each subject case, as output by the 2<sup>nd</sup> block process in Fig. 1.

Table 2. ECG noise sigma ( $\sigma$ ) figure determination, referred to SAECG, for Db4 optimal thresholding per case.

Case Number	1	2	3	4	5	6	7	8	9	10
Db4 Optimal Sigma ( $\sigma$ )	1.35	0.8	1.05	1.2	1.2	1.43	0.3	0.2	1.7	0.5

Using the optimal ECG noise sigma value for each case in Table 2, the Db4 threshold parameter was calculated using the same equations (Eqs.1 and 2) as in previous work [5].

$$Thr = x * \text{Sigma Noise} \quad (1)$$

$$\text{Where } x = \sqrt{2 * \text{Log}(n)} \quad (2)$$

with n being the number of data samples taken within the 8-minute ECG recording (sampling frequency = 2048 Hz) and after decimation by 10 (downsampled to 204.8 Hz).

## 2.3 HRV metrics processing

For HRV analysis, first a Pan-Tompkins Algorithm is applied autonomously and independently to both the standard chest ECG Lead I and to the bipolar Arm-ECG Lead-1 in order to detect QRS complexes, time-locate the ECG R waves [7] and generate the IBI of normal-to-normal beats time-series, used for HRV metrics correlation and linear regression analysis of Arm versus Chest ECGs.

Four clinically common HRV time-domain metrics are: the standard deviation of normal-to-normal IBI (SDNN), the RMS of the IBI values (RR-rms), the RR-median value of the IBI values and the interquartile-range value of normal-to-normal heartbeat intervals (IQRNN).

These four HRV metrics were measured systemically using Matlab signal processing software (ver. 2020R). Outlier subject case X-Y data-pair points were removed objectively using the Matlab command: `rmoutliers`.

Scatter plots of HRV metrics data pairs (Arm vs Chest) per subject case, were plotted using MS Excel software (Office 10 ver.), and the Pearson correlation coefficient, p

$$p = \frac{\sum_{i=1}^n (X_i - \bar{X})(Y_i - \bar{Y})}{\sqrt{\sum_{i=1}^n (X_i - \bar{X})^2} \sqrt{\sum_{i=1}^n (Y_i - \bar{Y})^2}} \quad (3)$$

(Eq. 3) and the scatter plots linear regression model (trendline) Coefficient of Determination ( $R^2$ ) were readily calculated with MS Excel available formulas facility.

### 3. Results

Ten subjects with similar upper arm circumferences were considered for this pilot study.

#### 3.1 Db4 optimised thresholding denoising

The novel 2-stage Daubechies Db4 wavelet denoising process, depicted in Fig.1, was implemented supported by the proposed adaptive SAECG-based optimal thresholding algorithm. The conventional Pan-Tompkins algorithm [7] was then run independently for the Chest Lead I (gold standard) and for the simultaneously recorded Arm-ECG Lead-1 QRS detection

Figure 2 shows the differences in chest ECG signal (black curve), the Absolute Arm-Lead1 ECG signal (black curve), Arm SAECG of Lead-1, using the SFP QRS alignment technique (red curve) [6], and Arm Lead1 after the proposed 2-stage Db4 denoising process (blue curve). Each Signal in Fig. 2 are the P-QRS-T in a 700 ms window.

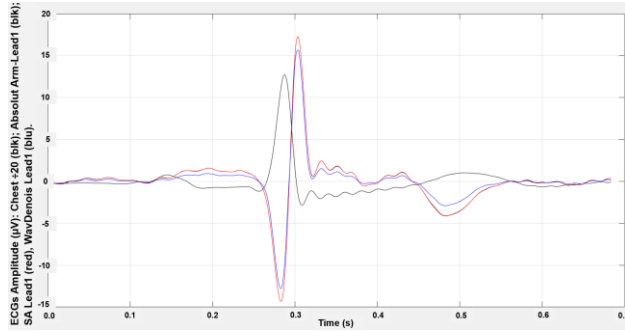


Figure 2. Chest ECG ÷ 20 µV (blak), Absolute Arm-Lead1 (blak), SA Lead1 (red), Wave-Denoised Lead1 (blu) 700 ms window.

Below in Fig.3, a comparison between Lead I Chest ECG, Arm-ECG before the 2-stage DB4 denoising process and after the applying the 2-stage DB4 denoising process. A significant reduction in noise can be seen in the Arm Lead-1 ECG signal after the Db4 denoising process. It can also be seen that before the 2-stage DB4 denoising was implemented the p-to-p Arm-ECG Lead-1 signal amplitude, is roughly 20 times smaller than that of the chest ECG shown in the top of the figure. This can be attributed to the arm ECG being recorded further from the signal source resulting in a smaller amplitude in comparison to the Chest ECG. Furthermore, after the Db4 denoising process was implemented, the arm ECG has

roughly a 10% loss in p-p amplitude in comparison to the arm ECG before the Db4 wavelet denoising process.

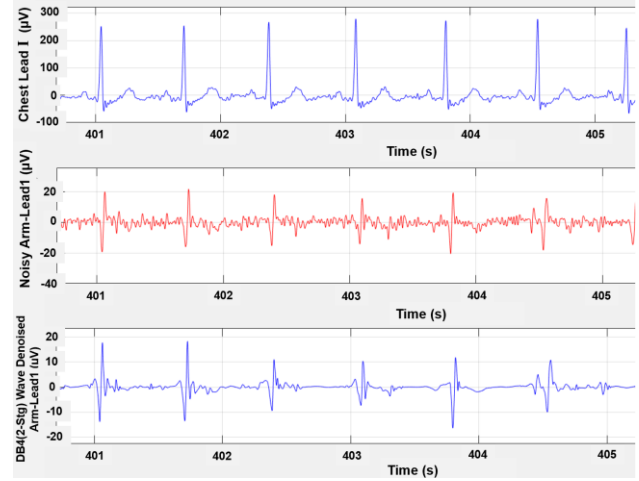
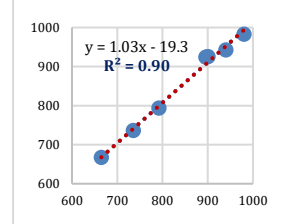


Figure 3. (Top) Chest ECG signal, (Middle) Noisy arm Lead-1 ECG before Db4, (Bottom) Clean ECG after Db4, all in µV.

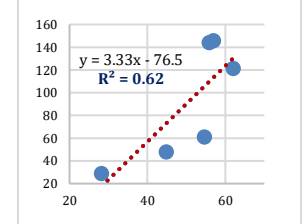
#### 3.2 Competitiveness of Arm-ECG HRV

HRV metrics were measured independently on the bipolar lead-1 Arm ECG after the 2-stage Db4 denoising process and correlated with HRV metric values measured on the standard chest ECG Lead I using the Pearson correlation coefficient ( $p$ ) and trendline Coefficient of Determination ( $R^2$ ). The results pair values data points per subject case scatter plots for the 4 HRV time domain metrics considered in this study, are shown in Fig.4, for (a) RR-rms, (b) SDNN, (c) RR-median and (d) IQRNN.

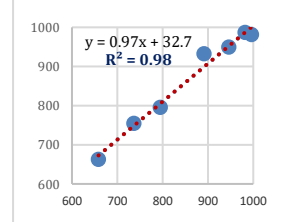
(a) RR-rms HRV metric: Arm-ECG Lead-1 vs standard chest Lead I measured values (ms), per subject case.



(b) SDNN HRV metric: Arm-ECG Lead-1 vs standard chest Lead I measured values (ms), per subject case.



(c) RR-median HRV metric: Arm-ECG Lead-1 vs standard chest Lead I measured values (ms), per subject case.



(d) IQRNN HRV metric: Arm-ECG Lead-1 vs standard chest Lead I measured values (ms), per subject case.

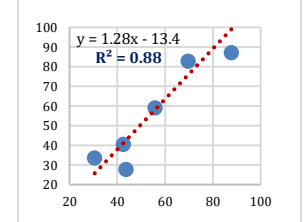


Figure 4. HRV metrics scatter plots (Arm-ECG Lead-1 vs Chest Lead I): (a) RR-rms (b) SDNN, (c) RR-median and (d) IQRNN.

The Pearson correlation ( $p$ ) between the arm-HRV-metrics measured values and HRV-metrics measured from the standard chest Lead I results were:  $p=0.789$ ,  $p=0.995$ ,  $p=0.991$  and  $p=0.940$ , and linear regression model coefficients of determination ( $R^2$ ) values (from scatter-plot of arm Lead-1 versus chest Lead I HRV values data point per subject) of:  $R^2=0.623$ ,  $R^2=0.991$ ,  $R^2=0.982$  and  $R^2=0.884$ , for SDNN, RR-rms, RR-median and IQRNN respectively. RR-rms and RR-median from the arm-ECG correlated well to measurements taken from the chest-ECG. SDNN with an  $R^2$  of 0.623 however may indicate an issue with ECG signal derived from the arm and prompts the need for further investigation.

#### 4. Discussion

Building on previous work (McCallan et al.) [5] on left-arm sensitivity and positive predictive value (PPV), looking at the ECG after the two-stage wavelet, in Figure 3, the standard chest Lead I ECG signal is shown as the “gold standard” signal compared to the arm Lead-1. After the 2-stage wavelet denoising process, there is clear reduction in the overall amplitude of the ECG, between the waves and the overall QRS complexes while remaining visible over the remaining background noise. Although all waves still seem to be in phase with one another. However, there could always be the potential that after denoising, you could remove some ECG waveform components, that could hinder with HRV measurements from the Arm-ECG.

On further inspection of the results from the earlier section, all metrics have an average of 3 outliers within the data, with RRSD being the exception with 4 pairs of data lying too ‘far’ from the general results, and are hence removed in Fig.4. The cause of outliers such as these could be a result of the range of ages and weights, which can contribute to the varying metrics, however all BMIs fall within the same range, so this is a less likely factor.

However, as well as the age and weight contributing to this, after the application of the Pan-Tompkins to both signals, it was found that less R waves were detected from the arm Lead-1 than from the Chest Lead I, an average of 50% less, which will affect all metrics. This affected a lot the SDNN HRV metric measured on the Arm-ECG, and this can be shown through the lowest correlation,  $p=0.789$ . This fact can also be backed up when looking at the linear regression model coefficients of determination of the metrics. Although all is positive, the lowest one comes from the SDNN at  $R^2=0.623$ . Although it is a lower result compared to the rest of the results, it is still a good correlation indicator to the Chest Lead I. This lends further to the conclusion that there is a feasibility to the Arm ECG metric measurements, using this technique, which is also used by Fariha [7] which produced similar results. The reduction in R waves within the arm Lead-1 can possibly be attributed to the decrease in the amplitude, due to the recording being further away than the heart electrical

source (far-field), leading to R waves that cannot be discerned from the rest of the noisy ECG waveform.

Observing the results of Figure 2, they reveal that the Arm-ECG that has been denoised using a Db4 wavelet process (blue curve), has the same timings as the Arm-ECG after a signal averaging process only (no Db4 filtering, red curve). The only difference between these two processes being the slight decrease in amplitude of the wavelet denoised ECG. This shows that there could be an opportunity for further comparison in a future study.

#### 5. Conclusion

With the results presented, it is fair to conclude due to all positive Pearson correlations, showing that the Arm Lead-1 has good correlation to the standard Chest Lead I, it’s feasible that the use of Arm Lead-1 as a standalone approach, using both the 2-stage wavelet denoising process and the Pan-Tompkins algorithm, have potentials for being used for long-term HRV monitoring and being attractive on a clinical scale, as all metrics resulted in a positive Pearson correlation and positive linear regression model coefficients compared with values from the Chest Lead I.

#### References

- [1] British Heart Foundation (2022). Facts and Figures; website (last visited on 18/Aug 2022): <https://www.bhf.org.uk/what-we-do/news-from-the-bhf/contact-the-press-office/facts-and-figures>
- [2] Propper, et al. (2020). The Wider Impacts of the Coronavirus Pandemic on the NHS (UK). Fiscal Studies, The J. of Applied Public Economics, 41(2). doi:10.1111/1475-5890.12227.
- [3] Hua, Z., Chen, C., Zhang, R., et al. (2019). Diagnosing Various Severity Levels of Congestive Heart Failure Based on Long-Term HRV Signal. Applied Sciences, 9(12), p.2544.
- [4] Shoushan, M.M., Reyes, B.A., Rodríguez, A.R.M. and Chong, J.W., (2022). Contactless Monitoring of Heart Rate Variability During Respiratory Maneuvers. IEEE Sensors Journal, 22(14), pp.14563-14573
- [5] McCallan, N. et al. (2019). Wearable Technology: Signal Recovery of Electrocardiogram From Short Spaced Leads in the Far-Field Using Discrete Wavelet Transform Based Techniques. In *2019 Computing in Cardiology*, IEEE.
- [6] Escalona, O.J. et al. (1993). A Fast and Reliable QRS Alignment Technique for High-Frequency Analysis of the Signal-Averaged ECG. Medical and Biol. Eng. and Computing, v.3, pp. S137-S146.
- [7] Fariha, M.A.Z., et al. (2020). Analysis of Pan-Tompkins Algorithm Performance with Noisy ECG Signals. Journal of Physics, doi:10.1088/1742-6596/1532/1/012022.
- [8] Brito, N.B. et al. (2016). Relationship Between Mid-Upper Arm Circumference and Body Mass Index in Inpatients, PLOS ONE, v.11(8), doi: 10.1371/journal.pone.0160480.

Address for Correspondence:

Name: Omar J Escalona.

Address: Ulster University, Shore Road, Newtownabbey, BT37 0QB, United Kingdom.

E-mail address: [oj.escalona@ulster.ac.uk](mailto:oj.escalona@ulster.ac.uk)